3. Results

3.1. Generation of an Lbx1^{GFP} mutant allele

Previous studies showed that *Lbx1* is expressed in long-range migrating but not in other types of muscle precursors during development (Jagla et al. 1995). To visualize migrating muscle precursors in the living embryo and to allow their isolation by FACS sorting, I generated a mutant *Lbx1* allele in which the coding sequence of green fluorescent protein (GFP) was fused to the initiating codon of the *Lbx1* gene.

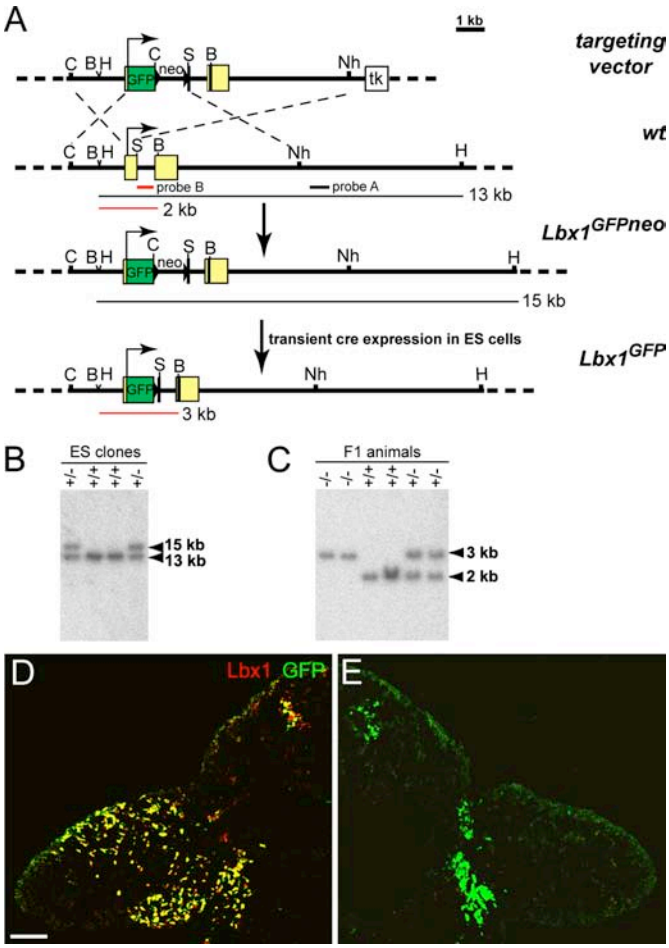

Figure 4. Generation of the *Lbx1^{GFP}* mutant allele. (A) Schematic representation of the targeting vector, the wild-type *Lbx1* locus and the mutated *Lbx1* allele before and after removal of the *neomycin* (neo) cassette using transient expression of *Cre* recombinase in ES cells. Exons in the *Lbx1* gene are depicted by yellow boxes. In the *Lbx1^{GFP}* allele, the first exon was exchanged by a *GAP43-GFP* cassette (green box); in addition, a frame-shift mutation (indicated by a black line) was introduced into the second exon. The targeting vector contains *neomycin* (neo) and *thymidine kinase* (tk) cassettes that were used for positive and negative selection, respectively. The positions of the probe A and probe B used for Southern analysis are shown by black and red bars, respectively, as well as the predicted fragment sizes obtained after Hind III (H) and Bam HI (B) digestion of genomic DNA (black and red lines, respectively). In addition, the following restriction enzyme sites are indicated C: Cla I; S: Sse8387 I; Nh: Nhe I. (B) Southern blot analysis of Hind III digested genomic DNA from wild-type and *Lbx1$^{GFP/+}$* ES cells using probe A for hybridization. (C) Southern blot analysis of Bam HI digested genomic DNA from wild-type, *Lbx1$^{GFP/+}$* and *Lbx1$^{GFP/GFP}$* F1 animals using probe B for hybridization. (D,E) Immunohistological analysis of forelimb sections of *Lbx1$^{GFP/+}$* and *Lbx1$^{GFP/GFP}$* embryos at E10 stained with anti-Lbx1 (red) and anti-GFP (green) antibodies. Bar: 125 µm.

The *Lbx1* gene consists of two exons. In the targeting vector, a *GAP43-GFP* cassette substituted the first exon of *Lbx1*; in addition, a small sequence containing a stop

codon was inserted into the homeobox located in the second exon of *Lbx1*, which resulted also in a frame-shift mutation. After recombination, this vector is expected to generate a mutant *Lbx1* locus that cannot produce functional Lbx1 protein; instead a GFP protein is made that is directed to the membrane. In addition, the *Thymidine kinase* gene and *Neomycin* gene flanked by loxP sites were included in the targeting vector. This allows a selection for cells that have introduced the vector into the genome by homologous recombination (Fig. 4A). The mutated *Lbx1* allele was electroporated into ES cells. I screened ES cell clones for homologous recombination events using Southern analysis (Fig. 4B). To excise the *Neomycin* cassette, $Lbx1^{GFPneo/+}$ ES cells were transfected with a *Cre*-recombinase expressing construct and $Lbx1^{GFP/+}$ clones were identified by Southern analysis. These ES cells were then used to generate an $Lbx1^{GFP/+}$ mouse strain (Fig. 4C). I analyzed the distribution of GFP^+ and $Lbx1^+$ cells in embryos that carry one copy of the $Lbx1^{GFP}$ allele, and observed GFP protein co-expressed with the endogenous Lbx1 protein in migrating muscle precursors (Fig. 4D). $Lbx1^{GFP/+}$ animals were crossed to obtain $Lbx1^{GFP/GFP}$ mutant embryos. No Lbx1 protein was detected in the limb of $Lbx1^{GFP/GFP}$ embryos by immunohistology using anti-Lbx1 antibodies (Fig. 4E). Moreover, changes in the distribution of muscle precursor cells were noted, which were identical to those described previously (Fig. 4D, E; (Brohmann et al. 2000)). The newly established $Lbx1^{GFP/+}$ mouse strain was used to isolate muscle precursor cells.

3.2. Isolation and expression profiling of muscle precursor cells from $Lbx1^{GFP/+}$ and $Lbx1^{GFP/GFP}$ embryos

GFP^+ muscle precursors were isolated from the limb bud of $Lbx1^{GFP/+}$ and $Lbx1^{GFP/GFP}$ mutant embryos. For this, the forelimbs of E10.5 embryos were dissected, dissociated and cells were filtered through a 70 µm cell strainer to obtain a single cell suspension. Before FACS sorting, cells were stained with propidium iodide, a DNA intercalating agent. The intact plasma membrane is not permeable to propidium iodide. Thus, only dead cells with a damaged plasma membrane are stained with propidium iodide and can therefore be excluded during cell sorting. Propidium iodide-negative, GFP-positive cells were isolated by flow cytometry (Fig. 5). The FACS sorting was performed at the FACS unit of the Rheumaforschungszentrum, Berlin.

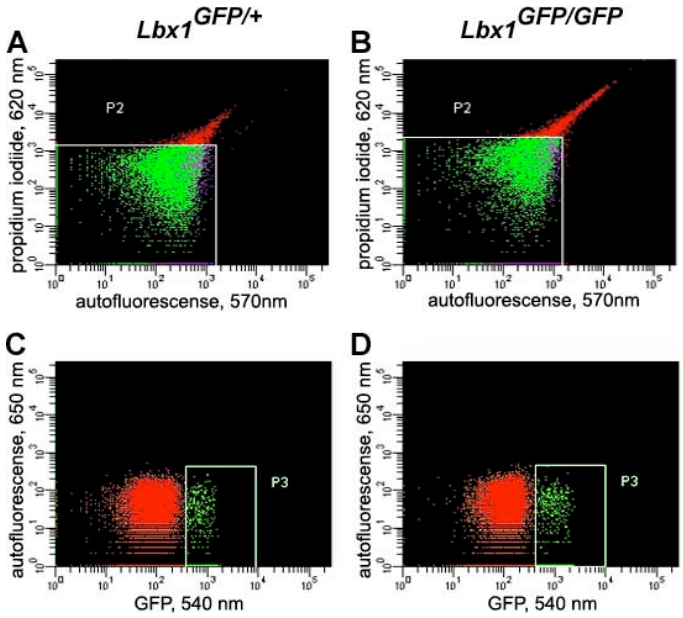

Figure 5. FACS sorting of *Lbx1*$^{GFP/+}$ and *Lbx1*$^{GFP/GFP}$ muscle precursor cells.
(A, B) FACS plots obtained after sorting of the initial cell population. A 488 nm-laser was used for excitation. Fluorescent signals at 620 nm (propidium iodide) and 570 nm (autofluorescense) were detected and the propidium iodide-negative population was selected as shown (gate P2 in A, B). (C, D) FACS plots obtained after sorting of the selected propidium iodide-negative population. 488 nm- and 635 nm-lasers were used for excitation and fluorescent signals at 540 nm (GFP) and at 650 nm (autofluorescense), respectively, were detected. Cells that were GFP-positive (gate P3 in C, D) were collected. X- and Y-axis represent the logarithmic scale of the signal intensities detected.

Total RNA from the sorted cells was isolated and used to generate biotin-labeled cRNA probes. Because of the limited amount of RNA isolated, I used a two-step amplification protocol to generate the hybridization probes (for details see Material and Methods). cRNA probes from three independent cell pools of both, *Lbx1*$^{GFP/+}$ and *Lbx1*$^{GFP/GFP}$ cells, were used to hybridize MGU74A/B/Cv2 Affymetrix GeneChips. An image analysis of the hybridized Affymetrix GeneChips was used to obtain hybridization intensity values. To analyze these values statistically, the Microarray Suite (MAS) 5.0 software was used. The intensities of the hybridization signal of the genes were evaluated. An average detection p value was used to assign a "present" or "absent" calls to a hybridization signal. Changes in expression levels were judged by the average change p value and the fold change value. The average detection p value was calculated using the MAS5.0 statistical algorithm; this includes a comparison of the intensity values of one group (*Lbx1*$^{GFP/+}$ or *Lbx1*$^{GFP/GFP}$) of hybridizations with the intensity values of a set of probes that detect the expression of housekeeping genes. A gene was assessed as being expressed (present) if its detection p value was equal or less than 0.02, as being expressed marginally if its p value is between 0.02

and 0.06, and as being not expressed (absent) if its detection p value was equal or higher than 0.06. Changes in gene expression were judged by the average change p value, which was calculated by applying a pair-wise Student's t-test in which the intensity values of different groups ($Lbx1^{GFP/+}$ versus $Lbx1^{GFP/GFP}$) were cross-compared. An average change p value equal to 0.5 reflects no change in gene expression; a gene was judged to be downregulated if average change p value was less than 0.25 and upregulated if average change p value was higher than 0.75. The fold change was calculated as a ratio of the average hybridization intensities of $Lbx1^{GFP/+}$ versus $Lbx1^{GFP/GFP}$ probes.

3.3. Analysis of genes expressed in *Lbx1*$^{GFP/+}$ muscle precursor cells

The MGU74A/B/Cv2 Affymetrix GeneChips allow the analysis of the expression of 36700 different sequences, 4500 of which were identified as being expressed in $Lbx1^{GFP/+}$ muscle precursor cells (detection p value ≤ 0.02). Identified sequences were annotated using Affymetrix Netaffx, NCBI, Ensemble and PubMed databases. The reliability of the data obtained from Affymetrix GeneChip analysis was verified. For this, I analyzed the expression of approximately 50 genes showing "present" calls by *in situ* hybridization or by searching for published expression patterns in the PubMed database. Such analysis reveals that 48 out of 50 analyzed genes were indeed expressed in muscle precursors, which validated the efficacy of the Affymetrix gene expression profiling. Large number of genes expressed in muscle precursors encodes integral membrane proteins and transcription factors that are summarized in Table1 and Table 2, respectively.

The expression profiling of $Lbx1^{GFP/+}$ muscle precursor revealed many genes that were reported previously being expressed and functionally important for the development of muscle precursors. For instance, *c-Met* and *Pax3* are expressed in muscle precursors at early stages and are essential for delamination and migration of these cells (Table 1,2; (Daston et al. 1996; Dietrich et al. 1999)). *Six1*, *Dach1* and *Pitx2* promote proliferation of muscle precursor cells (Table 2; (Kioussi et al. 2002; Li et al. 2003)). *Mox2* and *Mef2* were previously implicated in the control of differentiation of muscle precursors (Table 2; (Mankoo et al. 1999; Wang et al. 2001)).

Table1. Genes encoding integral membrane proteins that are expressed in *Lbx1*$^{GFP/+}$ muscle precursor cells, as determined by microarray analysis.

Affy_ID	Gene symbol	Gene	Detection p value
98169_s_at	***Fzd3***	Frizzled homolog 3, (Drosophila)	0.0005
139426_r_at	***Fgfr1***	Fibroblast growth factor receptor 1	0.003
93090_at	***Fgfr2***	Fibroblast growth factor receptor 2	0.006
95117_at	***Igf2r***	Insulin-like growth factor 2 receptor	0.004
108468_at	***Bmpr1a***	Bone morphogenetic protein receptor, type 1A	0.002
106644_at	*Tgfbr1*	Transforming growth factor, beta receptor I	0.0004
104188_at	*Notch2*	Notch gene homolog 2, (Drosophila)	0.0004
102250_at	*Il27ra*	Interleukin 27 receptor, alpha	0.002
102794_at	***CXCR4***	Chemokine (C-X-C) receptor 4	0.002
137077_at	*CXCR5*	Chemokine (C-X-C) receptor 5	0.003
93430_at	***Cmkor1***	Chemokine orphan receptor 1	0.006
114749_at	*Gpr23*	G protein-coupled receptor 23	0.0003
97004_at	*Olfr71*	Olfactory receptor 71	0.013
109757_at	***Edg3***	Endothelial differentiation G-protein-coupled receptor 3	0.011
117151_at	***c-Met***	Met proto-oncogene tyrosine kinase	0.0007
133639_r_at	***Ror2***	Receptor tyrosine kinase-like orphan receptor 2	0.012
160480_at	*Ptprs*	Protein tyrosine phosphatase, receptor type, S	0.0002
160760_at	*Ptprk*	Protein tyrosine phosphatase, receptor type, K	0.006
104673_at	***EphA4***	Eph receptor A4	0.02
98446_s_at	*EphB4*	Eph receptor B4	0.0002
160857_at	***Efnb2***	Ephrin B2	0.0004
95387_f_at	*Sema4b*	Semaphorin 4B	0.0004
102852_at	***Cdh2***	Cadherin 2	0.0002
162097_r_at	*Cdh3*	Cadherin 3	0.018
129896_at	***EST***	*Homolog of Protocadherin 17 (*Homo sapiens*)*	0,014
166351_f_at	*Pcdh18*	Protocadherin 18	0,001
100124_r_at	*Itgb1*	Integrin beta 1	0.0002
95292_at	***Itga4***	Integrin alpha 4	0.010
94117_f_at	***Punc***	Putative neuronal cell adhesion molecule	0.0002
100153_at	***Ncam***	Neural cell adhesion molecule	0.0002
100977_at	*Glycam1*	Glycosylation dependent cell adhesion molecule	0.001
92558_at	***Vcam1***	Vascular cell adhesion molecule 1	0.002
162677_at	*Fath*	fat tumor suppressor homolog (Drosophila)	0.0002
93604_f_at	*Igsf4*	Immunoglobulin superfamily, member 4	0.0002

The detection p values were calculated using Affymetrix MAS5.0 software. Genes whose expression in migrating muscle precursor cells was verified by *in situ* hybridization or had been reported previously are indicated in bold.

Moreover, this analysis revealed the number of genes whose expression in muscle precursors was not previously reported. For instance, *EphA4* and *Efnb2* that encode an Eph tyrosine kinase receptor and ligand for Eph receptors, respectively, show prominent expression in muscle precursor cells (Table 1; Fig. 6A-D). Interestingly, expression of these two genes is evidently restricted only to particular subpopulations of muscle precursor cells. For instance, *Efnb2* expression is observed in the dermomyotome and in the cells that compose the dorsal muscle mass in the limb at

E10.5 (Fig. 6A). Later in development, faint *Efnb2* expression is observed also in the cells of ventral muscle mass (Fig. 6B). *EphA4* expression is found in the myotome, the ventral lip of the dermomyotome and in the cells that are located in the close proximity of the dermomyotome. Very few cells that have already migrated into the limb were positive for *EphA4* suggesting that *EphA4* is expressed only in the cells that undergo delamination and shortly after it (Fig. 6C,D). *FoxM1* that encodes forkhead box transcription factor is expressed in myotome, limb mesenchyme and in muscle precursor cells. However, the expression of *FoxM1* is restricted to a population of muscle precursors that colonize the proximal ventral limb (Table 2; Fig. 6C).

Table2. Genes encoding transcription factors that are expressed in *Lbx1*$^{GFP/+}$ muscle precursor cells, as determined by microarray analysis.

Affy_ID	Gene symbol	Gene	Detection p value
99042_s_at	***Shox2***	Short stature homeobox 2	0.0002
101430_at	*Sox4*	SRY-box containing gene 4	0.0002
93669_f_at	*Sox11*	SRY-box containing gene 11	0.0002
94325_at	***Pbx1***	Pre B-cell leukemia transcription factor 1	0.0006
169259_f_at	***Six1***	Sine oculis-related homeobox 1 homolog (Drosophila)	0.0002
102788_s_at	***Pitx2***	Paired-like homeodomain transcription factor 2	0.01
99937_at	***Mox2***	Mesenchyme homeobox 2	0.0004
93852_at	***Mef2***	Myocyte enhancer factor 2A	0.015
100697_at	***Pax3***	Paired box gene 3	0.006
101526_at	***Msx1***	Homeo box, msh-like 1	0.002
107536_at	*Foxp1*	Forkhead box P1	0.0003
107523_at	***FoxM1***	Forkhead box M1	0.017
92958_at	*Foxo3a*	Forkhead box O3a	0.0002
101973_at	*Cited2*	Cbp/p300-interacting transactivator, with Glu/Asp-rich carboxy-terminal domain, 2	0.0002
95033_at	*Jmjd1a*	jumonji domain containing 1A	0.0002
94973_at	*Jmjd1b*	jumonji domain containing 1B	0.0002
114659_at	*Hbp1*	high mobility group box transcription factor 1	0.0003
101913_at	*Hey1*	Hairy/enhancer-of-split related with YRPW motif 1	0.0003
101902_at	*Rbpsuh*	Recombining binding protein suppressor of hairless (Drosophila)	0.0015
93057_at	*Btf3*	Basic transcription factor 3	0.0005
103959_at	*Phf13*	PHD finger protein 13	0.0008
96707_at	*Zipro1*	Zinc finger proliferation 1	0.0002
99052_at	*Zfhx1a*	Zinc finger homeobox 1a	0.0004
160848_at	*Zhx1*	Zinc fingers and homeoboxes protein 1	0.002
100941_at	*Miz1*	Msx-interacting-zinc finger	0.008
98122_at	*Lmo4*	LIM only 4	0.002

The detection p values were calculated using Affymetrix MAS5.0 software. Genes whose expression in migrating muscle precursor cells was verified by *in situ* hybridization or had been reported previously are indicated in bold.

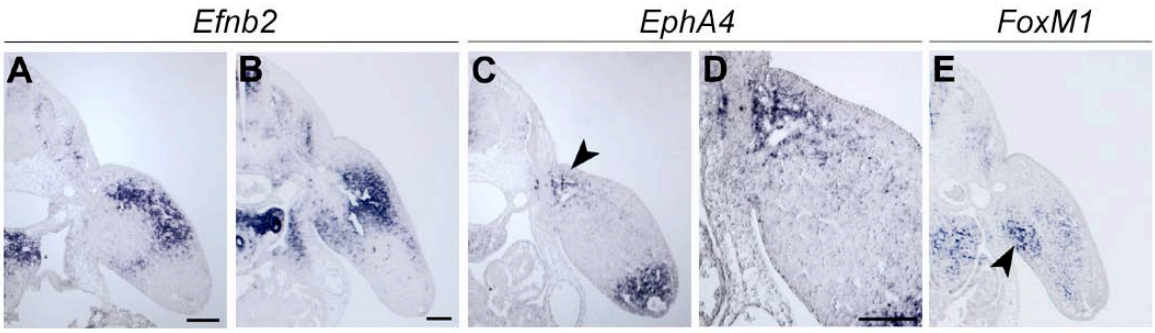

Figure 6. Expression of *Epnb2*, *EphA4* and *FoxM1* in the limb of wild type mouse embryos.
(A-E) *In situ* hybridization of mouse embryos at E10.5 (A, C, D) and at E10.75 (B, E) using probes specific for *Epnb2* (A, B), *EphA4* (C, D) and *FoxM1* (E). Bar: 125 µm.

Other surface molecules that were identified as being expressed in muscle precursor cells are the chemokine receptors *CXCR4* and *CXCR5*, orphan receptor *Cmkor1* and gene encoding a protocadherin that is closely related to the human *Pcdh17* (Table1; Fig. 7C,E and data not shown). *CXCR4* and *Pcdh17* are present in muscle precursors of both dorsal and ventral muscle masses, but again the expression pattern of these genes in the limb does not completely reproduce the pattern observed with *Lbx1* that is expressed in all hypaxial migrating muscle precursors. Thus, in contrast to the previously described genes like *Pax3*, *Lbx1*, *c-Met*, which are expressed in all migrating muscle precursors, my analysis revealed a set of genes that are expressed in restricted subpopulations. The expression of various genes in different cell subpopulations of muscle precursors might reflect previously unrecognized complexity in the regulation of their properties.

3.4. Analysis of genes differentially expressed in *Lbx1*$^{GFP/+}$ and *Lbx1*$^{GFP/GFP}$ muscle precursor cells

To identify genes regulated by the homeodomain transcription factor Lbx1, the gene expression profile of *Lbx1*$^{GFP/+}$ cells was compared to that of *Lbx1*$^{GFP/GFP}$ cells. Approximately 100 genes displayed deregulated expression in *Lbx1*$^{GFP/GFP}$ muscle precursors. 30 genes showed a change in the expression from “present” in *Lbx1*$^{GFP/+}$ cells (detection p value ≤0.02) to “absent” in *Lbx1*$^{GFP/GFP}$ cells (detection p value ≥ 0.06) or were downregulated more than 2-fold. About 70 genes showed were upregulated more than 2-fold or changed their expression from “absent” in *Lbx1*$^{GFP/+}$

cells (detection p value ≥ 0.06) to "present" in *Lbx1*$^{GFP/GFP}$ cells (detection p value ≤ 0.02). A selection of these genes is represented in Table 3.

Table 3. Genes differentially expressed in *Lbx1*$^{GFP/+}$ and *Lbx1*$^{GFP/GFP}$ muscle precursor cells

Affy_ID	Gene symbol	Gene	Change in expression	Change p value
Receptors, Integral membrane proteins				
117151_at	*c-Met*	Hepatocyte growth factor receptor precursor	-3.11	0.0000
102794_at	*CXCR4*	Chemokine (C-X-C) receptor 4	P→A	0.032
139519_at	*Gabra2*	Gamma-aminobutyric acid (GABA-A) receptor, subunit alpha 2	-4.08	0.0001
95292_at	*Itga4*	Integrin alpha 4	P→A	0.2809
117096_at	EST	Homolog of Protocadherin 17, *PCDH17* (*Homo sapiens*)	P→A	0.0001
109757_at	*Edg3*	Endothelial differentiation G-protein-coupled receptor 3	2.58	0,9999
100435_at	*Edg2*	Endothelial differentiation G-protein-coupled receptor 2	2.11	1.0
Transcription factors				
113030_at	*Hoxa9*	Homeo box A9	P→A	0.0000
92970_at	*Hoxa10*	Homeo box A10	P→A	0.0001
104021_at	*Hoxa11*	Homeo box A11	-2.63	0.0005
99937_at	*Mox2*	Mesenchyme homeobox 2	-2.32	0.0000
166427_f_at	Tbx3	T-box transcription factor 3	3.70	0,9666
92895_at	*Sim1*	Single-minded homolog 1	2.48	0,9999
Signaling proteins				
130994_at	*Nkd2*	Naked cuticle 2 homolog (Drosophila)	P→A	0.2104
97498_at	*Fhl1*	Four and a half LIM domains 1	-3.09	0.0004
113851_at	Sema3d	Semaphorin 3D	5.50	1.0
166303_i_at	*Wnt5a*	Wingless-related MMTV integration site	3.70	1.0
109161_at	*Ppap2b*	Phosphatidic acid phosphatase type 2B	2.33	0,9995
98424_at	*Ptpn13*	Protein tyrosine phosphatase, non-receptor type 13	2.0	0,9991
ESTs				
96749_f_at	EST	Homolog of human *LEM3*	-4.37	0.0002
113940_at	EST	Homolog of human *LETMD1*, protooncogene protein p40	P→A	0.2481

The fold change and change p values were calculated using Affymetrix MAS5.0 software.
P→A: expression of the gene is changed from Present (detection p value ≤ 0.02) to Absent (detection p value ≥ 0.06).

Lbx1 was suggested to function as a transcriptional repressor (Gross et al. 2002; Müller et al. 2002). This is in line with my data, which show a greater number of genes upregulated in the absence of Lbx1. The expression pattern of selected 'downregulated' or 'upregulated' genes was analyzed by *in situ* hybridization. This showed that many of the 'downregulated' genes were indeed expressed in migrating

muscle precursors of control mice and downregulated in the *Lbx1*$^{GFP/GFP}$ animals (Fig. 8A-F). In contrast, I had more problems to validate the expression of 'upregulated' genes, and as yet I have not identified a gene that is indeed upregulated in the muscle precursors of the mutant mice.

Among the genes, which were absent or expressed at reduced levels in *Lbx1*$^{GFP/GFP}$ muscle precursor cells were genes that encode proteins functioning in cell adhesion, directed cell migration and differentiation. For instance, the integrin alpha 4 (Itga4) and integrin beta 1 (Itgb1) subunits heterodimerize to form an integrin receptor, which functions in cell-matrix adhesions. In *Lbx1*$^{GFP/GFP}$ mutant, *Itga4* expression is downregulated (Table 3), but the expression of *Itgb1* is not altered (Table 1). Protocadherins are important for the cell-cell adhesion (reviewed in (Frank and Kemler 2002). The expression of a novel gene, which has high homology to human protocadherin gene *PCDH17*, is dramatically decreased in muscle precursor cells of *Lbx1*$^{GFP/GFP}$ mutant (Table 3; Fig. 7C,D). In addition, *Fhl1* was strongly downregulated but still present in *Lbx1*$^{GFP/GFP}$ muscle precursors (Table3; Fig. 7A,B). *Fhl1* encodes the protein that might function in the signal transduction cascades downstream of the Notch receptor (Taniguchi et al. 1998).

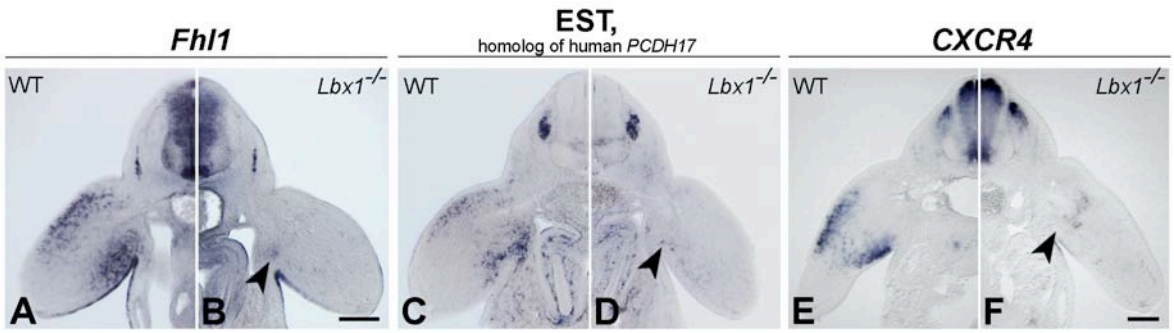

Figure 7. Expression of *Fhl1*, homolog of *PCDH17* and *CXCR4* in wild type and *Lbx1*$^{-/-}$ mouse embryos. (A-F) *In situ* hybridization of wild type (A, C, E) and *Lbx1*$^{-/-}$ (B, D, F) mouse embryos at E10.5 (A-D) and at E10.75 (E, F) using probes specific for *Fhl1* (A, B), *Pcdh17* (C, D) and *CXCR4* (E, F). Bars: 125 µm.

The microarray analysis also showed that chemokine receptor *CXCR4* is expressed in muscle precursor cells in the limb of wild type embryos but is lacking in *Lbx1*$^{GFP/GFP}$ muscle precursors (Table3, Fig. 7E,F). Over the last decade the function of *CXCR4* was intensively investigated. In different cell lineages, *CXCR4* was implicated in cell migration, motility and survival (for details and references see Introduction). In my

further work, I focused on an analysis of the *CXCR4* in the development of hypaxial muscle precursors.

3.5. Expression of *CXCR4* its ligand *SDF1* in mouse and chick embryos

SDF1 encodes the ligand for *CXCR4* receptor and its binding to the receptor is obligatory to elicit the CXCR4-mediated responses. I examined the expression of *CXCR4* and *SDF1* in chick and mouse embryos. *CXCR4* expressing cells are observed in the limb buds of chick and mouse embryos and were distributed in a pattern similar to that of *Pax3* or *Lbx1* expressing muscle precursor cells (Fig. 8A,C). CXCR4-expressing cells are also observed along the hypoglossal cord and in the mesenchyme of first branchial arch; this corresponds to the route and the target of those migrating precursor cells that generate tongue muscle (Fig. 8G). CXCR4 expression in muscle precursors that move towards the diaphragm is very low and therefore was not examined further (data not shown).

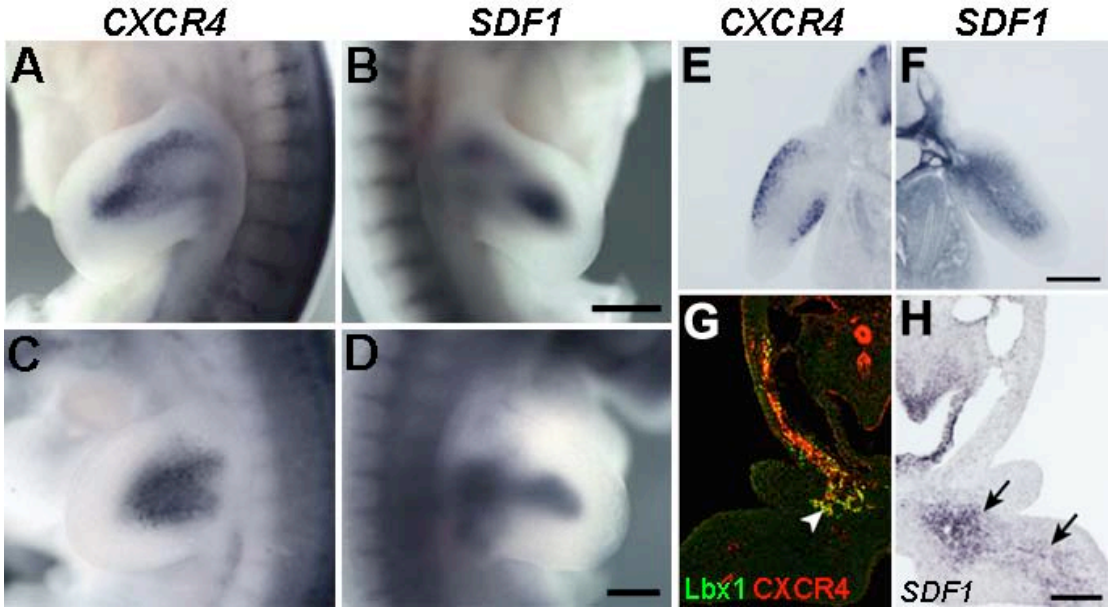

Figure 8. Expression of *CXCR4* and *SDF1* in mouse and chick embryos.
(A-F) *In situ* hybridization of chick embryos at HH25 (A, B) and mouse embryos at E10.25 (C-F) using probes specific for *CXCR4* (A, C, E) and *SDF1* (B, D, F). (G, H) Consecutive sections, displayed as mirror images, through the first branchial arch of wild-type mouse embryos at E10.25 were stained with antibodies against CXCR4 (red) and Lbx1 (green) (G) or hybridized with an *SDF1* specific probe (H). CXCR4 and Lbx1 were co-expressed in muscle precursors migrating towards the tongue anlage (arrowhead in G), whereas *SDF1* transcripts were detected in mesenchyme of the first branchial arch (arrows in H). Bars: (A, B) 500 µm; (C-H) 250 µm.

SDF1 expression was detected in the mesenchyme of the limb buds of chick and mouse embryos (Fig. 8B,D,F). The expression pattern of *SDF1* changes during development. At the time muscle precursor cells delaminate, *SDF1* is expressed in the proximal limb bud. After the cells entered the limb bud, *SDF1* is expressed broadly in the limb mesenchyme (Fig. 8F). A few hours later in development, *SDF1* expression in the proximal limb mesenchyme is reduced and *SDF1* transcripts become more abundant in the distal than the proximal limb (Fig. 8B,F and data not shown). *SDF1* transcripts are also detected in the mesenchyme of the first branchial arch (Fig. 8H). Thus, migrating muscle precursors, which express the CXCR4 receptor, are observed in the vicinity of SDF1-expressing cells in the limb buds of mouse and chick embryos. In the first branchial arch, SDF1 is expressed at the target of migrating cells that move to the tongue anlage.

To determine whether CXCR4 and Lbx1 mark identical or different cell populations, the expression patterns of Lbx1 and CXCR4 were compared by immunohistochemistry. Lbx1 appears in muscle precursors prior to their delamination from the ventral dermomyotome. In contrast, CXCR4 protein was not detectable in the ventral lip of the dermomyotome or in delaminating $Lbx1^+$ cells. However, CXCR4 and Lbx1 co-expression was observed in migrating precursor cells that had entered the limb bud at E10.25 (Fig. 9A). All $CXCR4^+$ cells in the limb are also $Lbx1^+$, demonstrating that CXCR4 is present in migrating muscle precursors. Nevertheless, not every $Lbx1^+$ cell in the limb bud expresses CXCR4, and differences in the distribution of these proteins were noted. For instance, $Lbx1^+CXCR4^+$ cells, which represent a small proportion of the entire muscle precursor pool at E10.25, are located closer to the ectoderm while $Lbx1^+CXCR4^-$ are found further centrally in the limb bud (Fig. 9A). Between E10.25 and E10.75, the number of $CXCR4^+$ cells increases, but even at this stage a significant number of $Lbx1^+CXCR4^-$ cells are detectable (Fig. 9B). CXCR4 and Lbx1 are also co-expressed in those muscle precursors that migrate towards the first branchial arch. Compatible with their expression pattern in the limb, not every $Lbx1^+$ cell in the hypoglossal cord is $CXCR4^+$, but compared to the limb bud the larger proportion of $Lbx1^+$ cells expresses CXCR4 (Fig. 8G). All $Pax3^+$ cells in the limb co-express Lbx1 (Gross et al. 2000). Consequently, analysis of the expression patterns of Pax3 and CXCR4 reveals that $Pax3^+CXCR4^+$ and $Pax3^+CXCR4^-$ cells exist in the limb.

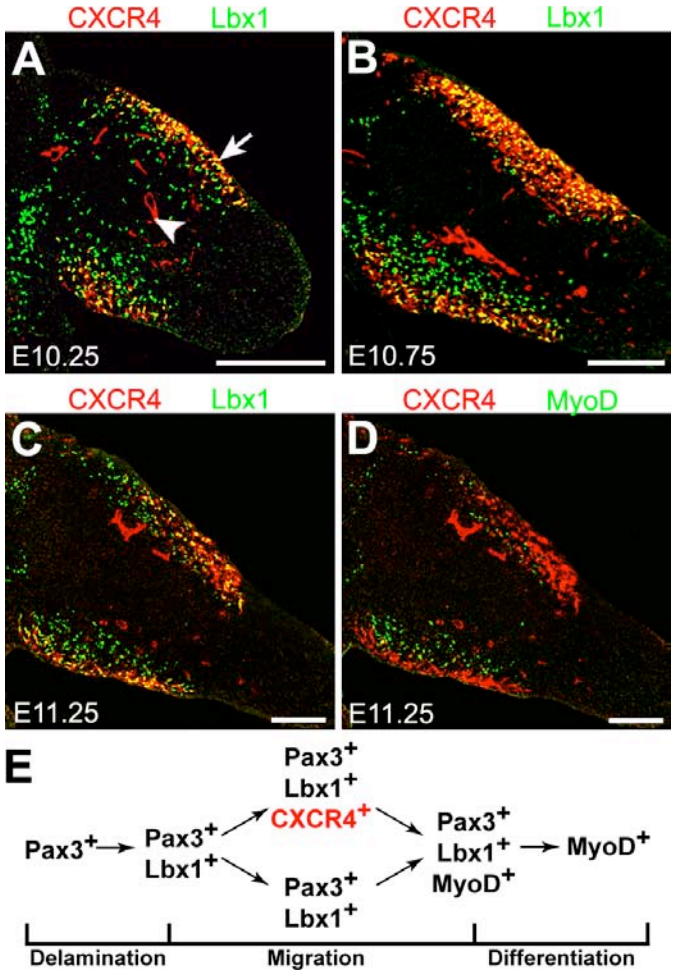

Figure 9. Expression of CXCR4, Lbx1 and MyoD in limb muscle precursors.
(A, B) Sections of the forelimb of E10.25 (A) and E10.75 (B) mouse embryos stained with anti-CXCR4 (red) and anti-Lbx1 (green) antibodies. CXCR4 and Lbx1 were co-expressed in some, but not all muscle precursor cells (arrow in A). In addition, CXCR4 was also present in limb endothelial cells (arrowhead in A). (B) At E10.75, the proportion of $Lbx1^+/CXCR4^+$ cells had increased in the limb. (C, D) Section of the forelimb of mouse embryo at E11.25 stained with anti-CXCR4 (red) (C, D), anti-Lbx1 (green) (C) and anti-MyoD (green) (D) antibodies. $CXCR4^+/MyoD^+$ double positive cells were very rare. (E) Schematic representation of gene expression in developing muscle precursors. CXCR4 expression is induced after muscle precursors have delaminated and have reached the limb, and is extinguished prior to their differentiation. Bars: 250 µm.

Analysis of CXCR4 and MyoD expression by immunohistochemistry revealed that very few $CXCR4^+$ cells co-express muscle differentiation factor MyoD (Fig. 9D). In addition, $CXCR4^+$ and $MyoD^+$ cells occupy different positions within the developing limb bud, i.e. $CXCR4^+$ cells locate closer to the ectoderm than $MyoD^+$ cells. Thus, CXCR4 is expressed in a subpopulation of muscle precursor cells that is distinct from differentiated, MyoD-positive myoblasts (Fig. 9C,D). In contrast, $MyoD^+Lbx1^+$ or $MyoD^+Pax3^+$ cells were frequently observed (Fig. 12A). These data indicate that muscle precursors do not express CXCR4 at the time when they are specified and

delaminate, but CXCR4 protein appears in the cells when they migrate. CXCR4^{+} cells co-express Lbx1 and Pax3, but not the muscle differentiation factor MyoD. CXCR4 is thus downregulated in muscle precursors prior to their differentiation (see Fig. 9E for a summary).

3.6. CXCR4 is expressed in muscle precursors of hypoglossal stream, but not of the limb in *Lbx1* mutant

CXCR4 was identified as a gene downregulated in muscle precursor cells that migrate into the limb bud in *Lbx1* mutant. Indeed, *CXCR4* transcripts were generally missing in limb muscle precursors of Lbx1$^{GFP/GFP}$ embryos (Fig. 7E,F). Consequently, no CXCR4 protein was observed in those muscle precursors that had entered the proximal-ventral limb of *Lbx1* mutant embryos (Fig. 10A,B). However, when muscle precursors that migrate toward the tongue anlage were analyzed, CXCR4 expression was observed in the hypoglossal stream of both wild type and *Lbx1*$^{-/-}$ embryos (Fig. 10C,D). Thus, the expression of *CXCR4* is not absolutely dependent on *Lbx1*.

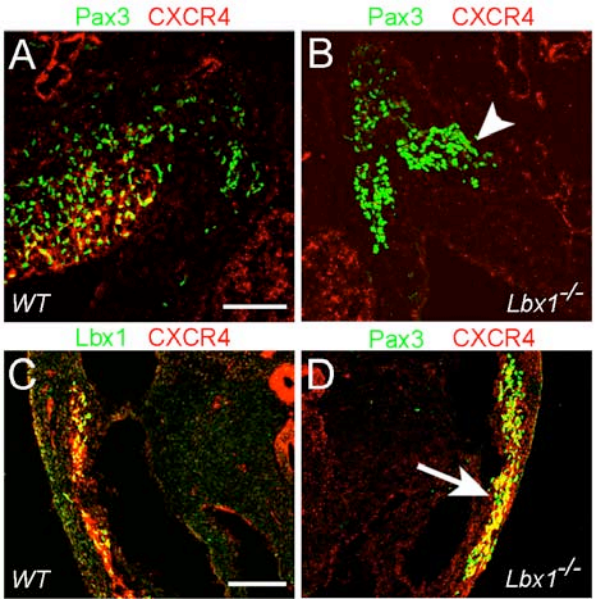

Figure 10. CXCR4 expression in muscle precursors of the limb and hypoglossal stream in wild-type and *Lbx1*$^{-/-}$ embryos. Sections of the forelimbs (A,B) and at the level of the first branchial arch (C,D) of wild type (A,C) and *Lbx1*$^{-/-}$ (B,D) embryos at E10.5 were analyzed with anti-Lbx1 (green) and anti-CXCR4 (red) (C) or with anti-Pax3 (green) and anti-CXCR4 (red) (A, B, D) antibodies. In control embryos, CXCR4 is expressed in muscle precursors of the limb and hypoglossal stream. Note, that CXCR4 is absent in Pax3^{+} cells in the limb (arrowhead in B), but is still expressed in Pax3^{+} cells of the hypoglossal stream (arrow in D). Bars: 125 µm.

3.7. Ectopic application of SDF1 in the chick limb attracts muscle precursor cells and delays their differentiation

SDF1 is expressed in the vicinity of the CXCR4-positive muscle precursors that colonize the limb bud and the first branchial arch. The correlation between *SDF1* expressing areas and the position of muscle precursors during migration and at the targets raises the possibility that SDF1 could influence the migration of $CXCR4^+$ muscle precursor cells. To examine this, SDF1 gain-of-function experiments were performed using SDF1-expressing cell transplantations in the chick. For this, COS1 cells were transiently co-transfected with SDF1-expressing and control constructs, or with a control construct alone (see Material and methods). 36 hrs after the transfection COS1 cells were harvested and cell aggregates were implanted into the right forelimb bud of chick embryos (HH19-20). The untreated left forelimb was used as a control. The muscle precursor cells in manipulated chick embryos were detected using *in situ* hybridization at HH24-25 with probes specific for *CXCR4*, *Pax3*, *MyoD* and *Myf5*.

In the limb of those embryos that received an implant of COS1 cells expressing SDF1, CXCR4-positive muscle precursors were observed at ectopic positions close to the implants (12 of 12 cases examined) (Fig. 11A-C). To further analyze the effect of ectopic application of SDF1, chick embryos were sectioned after whole-mount *in situ* hybridization using *CXCR4* specific probe and distribution of muscle precursor cells was assessed. This analysis reveals that CXCR4-positive muscle precursors indeed accumulated in the vicinity of SDF1 expressing implants; these cells, however, avoided to enter the limb mesenchyme, which is located more centrally (Fig. 11J-K). This data indicates that SDF1 can influence the migration of muscle precursors cells; it acts as a chemoattractant for CXCR4-positive muscle precursors. When the Pax3-positive population of muscle precursors was analyzed, a substantial redistribution of muscle precursor cells was also observed after SDF1-expressing cells were implanted (11 of 17 cases examined) (Fig. 11D-F). However, the effect on Pax3-positive muscle precursors was less pronounced. For instance, despite the fact that $Pax3^+$ cells aggregated around the implant, some $Pax3^+$ cells were observed in the limb bud at remote positions, which respect to the COS1 implant (Fig. 11E). This indicates that not all $Pax3^+$ respond to SDF1. My expression data indicate that not all Pax3-expressing muscle precursors co-express CXCR4. Thus, $Pax3^+CXCR4^-$ and

$Pax3^{+}CXCR4^{+}$ cell populations exist and $Pax3^{+}CXCR4^{-}$ cells are not expected to respond to ectopic SDF1 signals. As a control, implantation experiments were performed using COS1 cells transfected with GFP expression construct. None of the embryos that had received such an implant showed ectopically positioned muscle precursors when they were analyzed by *in situ* hybridization with a *CXCR4* specific probe (5 of 5 cases examined; data not shown).

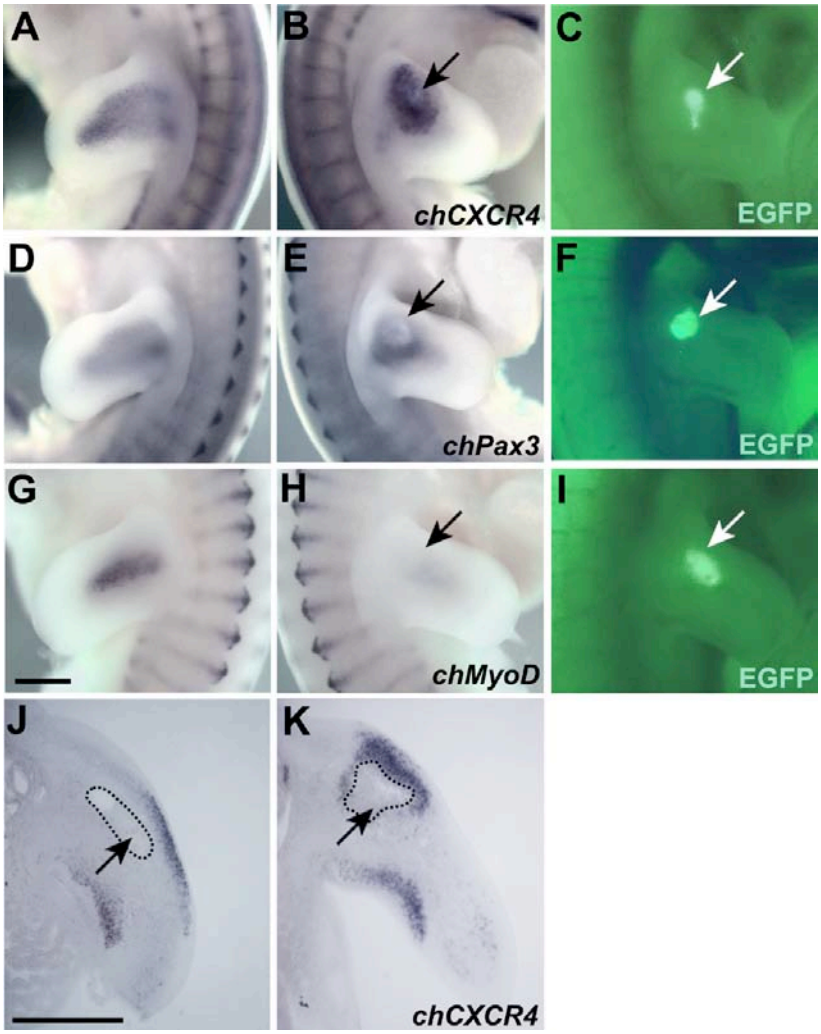

Figure 11. Muscle progenitors are attracted by an ectopic source of SDF1. COS1 cells co-transfected with SDF1 and GFP expression plasmids were implanted into the right wing bud of chick embryos at HH19-20. The distribution of muscle progenitor cells was analyzed at HH25 in the untreated (A, D, G) and treated contra-lateral limb (B, E, H) by *in situ* hybridization using *chCXCR4* (A, B), *chPax3* (D, E) and *chMyoD* (G, H) specific probes. The positions of the GFP positive implants are shown (C, F, I) and are also indicated by arrows. Note the aberrant position of the $CXCR4^{+}$ and $Pax3^{+}$ progenitor cells and the reduction of the MyoD signal in the limb implanted with SDF1 expressing cells. (J,K) COS1 cells transfected with GFP expression plasmid only (J) or COS1 cells co-transfected with SDF1 and GFP expression plasmids (K) were implanted into the limb bud, and the distribution of muscle progenitors was analyzed on sections after *in situ* hybridization using *chCXCR4*. The position of the implant is indicated. Bars: 500 µm.

To test the effect of ectopic SDF1 on differentiation of muscle precursors, transplanted chick embryos were hybridized with *MyoD* and *Myf5* probes. Compared to the untreated, contra-lateral limbs, the limbs that had received an implant of SDF1-producing cells displayed a significantly reduced *MyoD* (6 of 6 cases examined) or *Myf5* (5 of 5 cases examined) hybridization signal (Fig. 11G-I; data not shown). The expression of *MyoD* and *Myf5* was not changed when COS1 cells transfected with the control construct alone were implanted (5 of 5 cases examined; data not shown). These data show that muscle precursors respond to SDF1 signals during their migration. SDF1 can attract the CXCR4-positive muscle precursor cells and suppresses their differentiation.

3.8. Loss of CXCR4 affects the distribution and the number of muscle precursor cells

To investigate the effect of loss-of-function *CXCR4* mutation on the migration of hypaxial muscle precursors, the distribution of such cells was examined in mouse embryos that carry a mutation in the *CXCR4* gene. The *CXCR4* mutant allele was described previously (Ma et al. 1998). To visualize the muscle precursor cell population, the limb and branchial arch tissue of $CXCR4^{+/-}$ and $CXCR4^{-/-}$ embryos was stained with antibodies directed against Lbx1 and MyoD.

The ectopic application of SDF1 into the chick embryo limbs showed a strong effect on migration and differentiation of muscle precursor cells. However, loss of CXCR4 receptor affected the distribution of muscle precursors in the limb only in a mild manner. In particular, the number of muscle precursor cells located distally in the limb appears to be slightly reduced compared to control mice (Fig. 12A,B). To quantify this, the limb was divided into four domains, dorsal proximal, dorsal distal, ventral proximal and ventral distal, and the numbers of $Lbx1^+$ cells were determined in each domain (Fig. 12I). This analysis revealed that the number of muscle precursor cells in the dorsal limb of $CXCR4^{-/-}$ embryos at E10.75 was changed compared to control embryos (Fig. 12A-C). Moreover, the reduction in $Lbx1^+$ cell numbers was more pronounced in the distal (25%) than in the proximal domain (35%) of the dorsal limb (Fig. 12C, compare domain I and domain II). The number of $Lbx1^+$ cells in the ventral limb of $CXCR4^{-/-}$ embryos was not affected significantly (Fig. 12A-C).

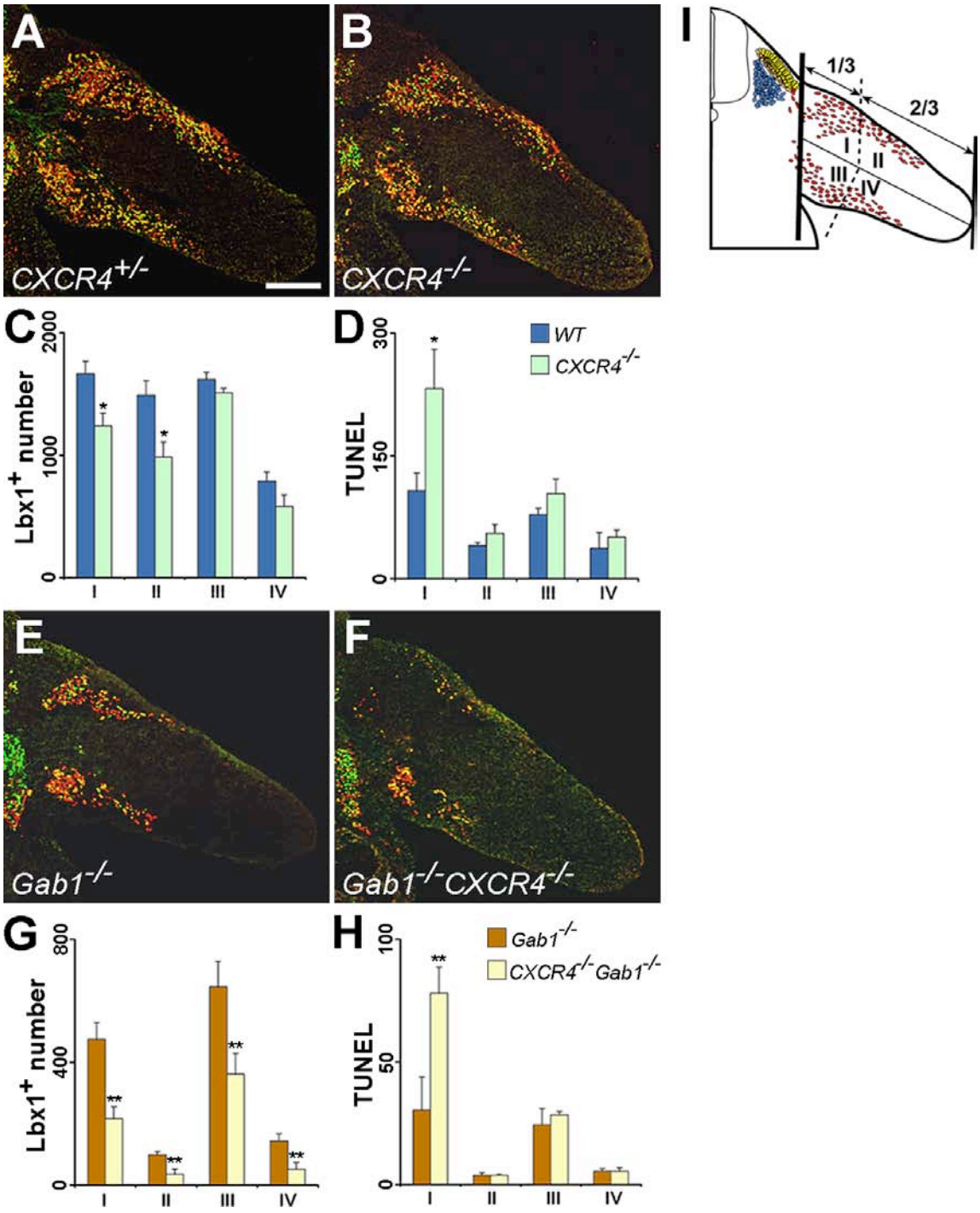

Figure 12. Distribution of muscle precursor cells in the limb.
(A-D) Sections of forelimbs of *CXCR4*$^{+/-}$ (A), *CXCR4*$^{-/-}$ (B), *Gab1*$^{-/-}$ (C) and *CXCR4*$^{-/-}$*Gab1*$^{-/-}$ (D) embryos at E10.75 were analyzed with anti-Lbx1 (red) and anti-MyoD (green) antibodies. (E-H) Quantification of the numbers of Lbx1^{+} and TUNEL^{+} cells located in distinct domains of forelimbs of embryos with the genotypes *CXCR4*$^{+/-}$ (blue bars) and *CXCR4*$^{-/-}$ (green bars), (E, F); *Gab1*$^{-/-}$ (orange bars) and *CXCR4*$^{-/-}$*Gab1*$^{-/-}$ (yellow bars), (G, H). For this, consecutive sections of E10.75 embryos were analyzed by immunohistochemistry, and the Lbx1^{+} or TUNEL^{+} cell numbers were counted on every third section in the different limb domains; *, p value < 0.007, n=5; **, p value < 0.005, n=4 (see also Material and Methods for further details). (I) Schematic drawing of a developing limb and the four domains defined therein: dorsal proximal (I), dorsal distal (II), ventral proximal (III) and ventral distal (IV). Bar: 250 µm.

Several mechanisms might account for the decrease in cell numbers, like impaired migration of muscle precursors, premature differentiation or impaired survival. To distinguish these possibilities, the differentiation, proliferation and cell death of muscle precursor cells were assessed. For this, $MyoD^+$, $Lbx1^+BrdU^+$ and $TUNEL^+$ absolute cell numbers were determined. Similar to the change in $Lbx1^+$ cell numbers, the number of $MyoD^+$ cells was reduced in the dorsal limb, and the distal domain was stronger affected than the proximal one. However, the differentiation rate, i.e. the number of $MyoD^+$ cells/number of $Lbx1^+$ cells, was not markedly altered (differentiation rate: control 59±3%; *CXCR4*$^{-/-}$ 50±4%, p value = 0.09). Proliferation of muscle precursors was analyzed using BrdU incorporation experiments. $Lbx1^+BrdU^+$ double positive cells were counted and proliferation rate was determined as $Lbx1^+BrdU^+$ cell number/$Lbx1^+$ cell number. Again, no significant change was observed in the proliferation rate of muscle precursor cells of *CXCR4*$^{-/-}$ and control embryos at E10.75 (proliferation rate: control 58±5%; *CXCR4*$^{-/-}$ 61±5%, p value = 0.18). Thus, differentiation and proliferation of muscle precursor cells are not considerably affected and therefore cannot be responsible for the reduced $Lbx1^+$ cell numbers in the dorsal limb of *CXCR4*$^{-/-}$ embryos. Cell death was analyzed by TUNEL staining (see Materials and methods for the detail). A considerable increase in apoptosis in the proximal but not in the distal domain of the dorsal limb was observed in *CXCR4*$^{-/-}$ mutants compared to control embryos (Fig. 12D, compare domains I and II). In conclusion, these data show that muscle precursor cells in the dorsal limb of *CXCR4*$^{-/-}$ mutant embryos are not correctly distributed, and that the survival of muscle precursors is impaired.

Gab1 encodes an adaptor molecule that mediates the downstream signals from the tyrosine kinase receptors, like c-Met. Previously it was reported that targeted mutation of *Gab1* impairs delamination of muscle precursor cells and also affects their migration (Sachs et al. 2000). I also analyzed the effect of the *CXCR4* mutation on a *Gab1* mutant background. For this analysis, *CXCR4*$^{-/-}$*Gab1*$^{-/-}$ and *CXCR4*$^{+/+}$*Gab1*$^{-/-}$ embryos were compared (Fig. 12E,F). In the dorsal and ventral limbs, the numbers of $Lbx1^+$ and $MyoD^+$ cells were further reduced in *CXCR4*$^{-/-}$*Gab1*$^{-/-}$ compared to *CXCR4*$^{+/+}$*Gab1*$^{-/-}$ embryos (Fig. 12E-G and data not shown). The proliferation of $Lbx1^+$ muscle precursor cells was not noticeably changed in the limb of *Gab1*$^{-/-}$ or

CXCR4$^{-/-}$*Gab1*$^{-/-}$ mice (proliferation rate: *CXCR4*$^{+/+}$*Gab1*$^{-/-}$ 56±4%; *CXCR4*$^{-/-}$*Gab1*$^{-/-}$ 53±5%, p value = 0.26). Moreover, no significant difference in proliferation was observed for limb muscle precursors between control and *CXCR4;Gab1* double mutant mice (proliferation rate: control 58±5%; *CXCR4*$^{-/-}$*Gab1*$^{-/-}$ 53±5%, p value = 0.21). Similarly, the differentiation rate was not markedly altered when *Gab1* single mutant and *CXCR4;Gab1* double mutant mice were compared (differentiation rate: *CXCR4*$^{+/+}$*Gab1*$^{-/-}$ 50±8%; *CXCR4*$^{-/-}$*Gab1*$^{-/-}$ 44±5%, p value = 0.36). However, a small but significant decrease in the differentiation rate of muscle precursor cell was observed in the limb of *CXCR4;Gab1* double mutant mice when they were compared to the control mice (differentiation rate: control 59±3%; *CXCR4*$^{-/-}$*Gab1*$^{-/-}$ 44±5%, p value = 0.03). The number of apoptotic cells in the areas occupied by muscle precursor cells was increased in the proximal domain of dorsal limb in *CXCR4;Gab1* double mutants compared to *Gab1* mutant mice (Fig. 12H).

CXCR4 is also expressed in muscle precursor cells that migrate to the first branchial arch to form intrinsic tongue muscle (Fig. 8G). Therefore the effect of *CXCR4* mutation on muscle precursors of the hypoglossal stream was assessed. In control embryos at E10.75, a stream of muscle precursors along the hypoglossal cord could be observed, and a large number of muscle precursor cells had reached the floor of the first branchial arch (Fig. 13A). The Lbx1^{+} or MyoD^{+} cell population that had reached the first branchial arch appears to be reduced in number in *CXCR4*$^{-/-}$ embryos compared to controls (Fig. 13A,B). Moreover, when the effect of the *CXCR4* mutation was analyzed on sensitized *Gab1*$^{-/-}$ background, the changes in the distribution of muscle precursor cells of the hypoglossal stream became more severe. In the *Gab1* mutant embryos, muscle precursors were observed along the hypoglossal stream and colonizing the mesenchyme of the first branchial arch, but despite this, the number of Lbx1^{+} or MyoD^{+} cells in the first branchial arch was lower than in control mice (Fig.13A,C). In *CXCR4;Gab1* double mutant embryos, the migrating muscle precursor cells were observed only along the migrating route but not at the target, i.e. Lbx1^{+} or MyoD^{+} cells were not detectable in the floor of the first branchial arch (Fig. 13D). Also at E11.5, I found no Lbx1^{+} or MyoD^{+} cells in the branchial arch of *CXCR4*$^{-/-}$*Gab1*$^{-/-}$ embryos (data not shown). Thus, in the *CXCR4;Gab1* double mutants the migrating cells are not only impaired, but fail to reach this target.

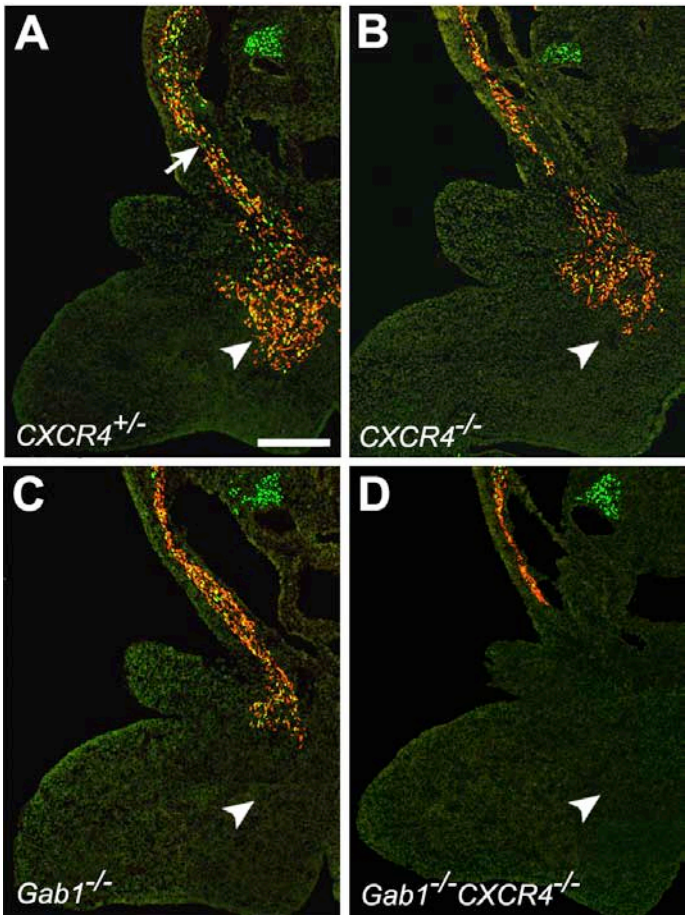

Figure 13. Migration of muscle precursors along the hypoglossal cord.
Sections of the first branchial arch of *CXCR4*$^{+/-}$ (A), *CXCR4*$^{-/-}$ (B), *Gab1*$^{-/-}$ (C) and *CXCR4*$^{-/-}$*Gab1*$^{-/-}$ (D) embryos at E10.75 were analyzed with anti-Lbx1 (red) and anti-MyoD (green) antibodies to identify muscle precursor cells. In control embryos, muscle precursors were observed along the hypoglossal cord (arrow) and colonized the mesenchyme of the first branchial arch, the target (arrowhead). Note the reduction in the numbers of muscle precursors in the first branchial arch of *CXCR4*$^{-/-}$ and *Gab1*$^{-/-}$ embryos, and their absence in *CXCR4*$^{-/-}$*Gab1*$^{-/-}$ embryos. Bar: 250 µm.

3.9. Effect of *CXCR4* mutation on the generation of skeletal muscle

To examine whether the changes in the numbers of muscle precursor cells affected the generation of differentiated skeletal muscle, tongue and limb muscle in control and *CXCR4*$^{-/-}$ mutant embryos were compared at E13.5. Skeletal muscles were visualized using anti-myosin and anti-MyoD antibodies (Fig. 14, 15). Despite the fact that the distal domain of dorsal limb was deprived of 35% of its muscle precursor pool at E10.75, the size and distribution of muscle groups in the lower forelimb were not markedly altered at E13.5 in *CXCR4*$^{+/-}$ and *CXCR4*$^{-/-}$ embryos (Fig. 14A,B). Analysis of differentiated skeletal muscle of hindlimbs also revealed no reproducible differences in muscle size between mutant and control embryos (data not shown). It appears that the reduction in the number of precursors at early developmental stages

was compensated subsequently and did not affect the final muscle size. The limb muscle of *CXCR4*$^{+/+}$*Gab1*$^{-/-}$ mutant mice was affected compared to control mice; both extensor and flexor muscle groups are reduced in size and particular muscles are missing (Fig. 14C). Flexor muscle groups were less affected in the lower forelimb of *Gab1* mutant mice, and only few muscles differed considerably from corresponding ones in the control mice.

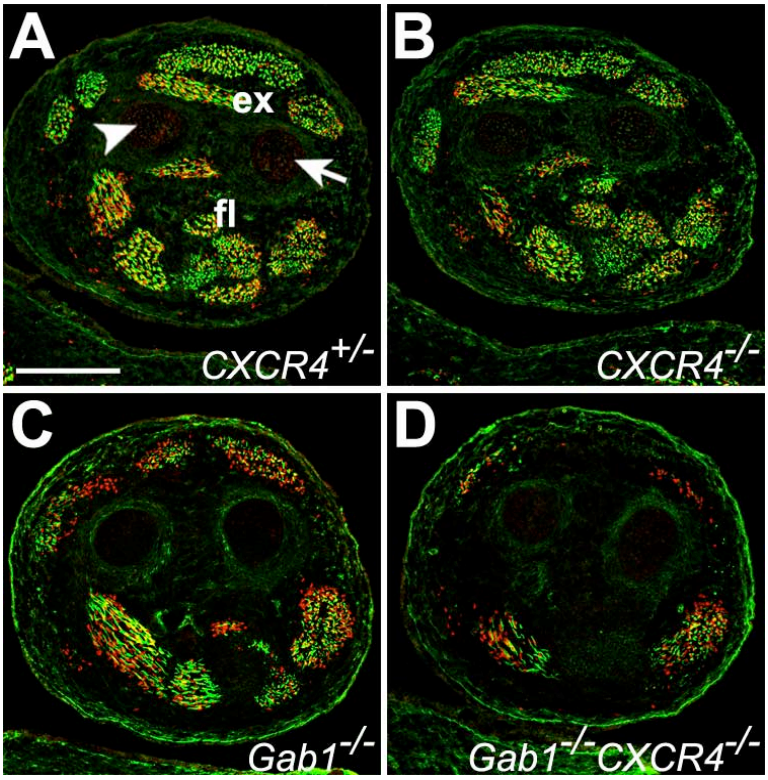

Figure 14. Differentiated muscle groups of the limb.
(A-D) Transverse sections through the proximal part of the lower forelimb of *CXCR4*$^{+/-}$ (A), *CXCR4*$^{-/-}$ (B), *Gab1*$^{-/-}$ (C) and *CXCR4*$^{-/-}$*Gab1*$^{-/-}$ (D) embryos at E13.5 stained with antibodies to myosin (green) and MyoD (red). Indicated are extensor (ex) and flexor (fl) muscles, arrowhead and arrow in E point towards the radius and ulna, respectively. Bars: 250 µm.

In *CXCR4;Gab1* double mutant embryos, the size of different muscle groups in the lower forelimb was further reduced and some muscle groups, especially extensor muscles, were lacking, even if these muscle groups were present in Gab1 single mutant mice (Fig. 14C,D). Thus, decreases in numbers of muscle precursors in *Gab1*$^{-/-}$ or *CXCR4*$^{-/-}$*Gab1*$^{-/-}$ at earlier stages leads to the decreased size or absence of different muscle groups, whereas the reduction in cell numbers caused by *CXCR4* mutation alone gives no reproducible effect on differentiated skeletal muscle.

The analysis of tongue muscle at E13.5 showed no major differences between *CXCR4*$^{-/-}$ and control mice (Fig. 15A,B). However, when the tongue muscles in *CXCR4*$^{-/-}$*Gab1*$^{-/-}$ and *CXCR4*$^{+/+}$*Gab1*$^{-/-}$ animals were compared, substantial differences were noted (Fig. 15C,D). In *Gab1* mutant mice, the intrinsic tongue muscle was smaller compared to control animals, but muscle fibers were present in both proximal and distal tongue (Fig. 15C). In contrast, the distal portion of the tongue of *CXCR4;Gab1* double mutants strongly affected (Fig. 15D). Thus, a fragment of the intrinsic tongue muscle was present in the proximal, but not in the distal tongue. As a result, the overall size of the tongue was very small in *CXCR4;Gab1* mutant embryos (Fig. 15C,D).

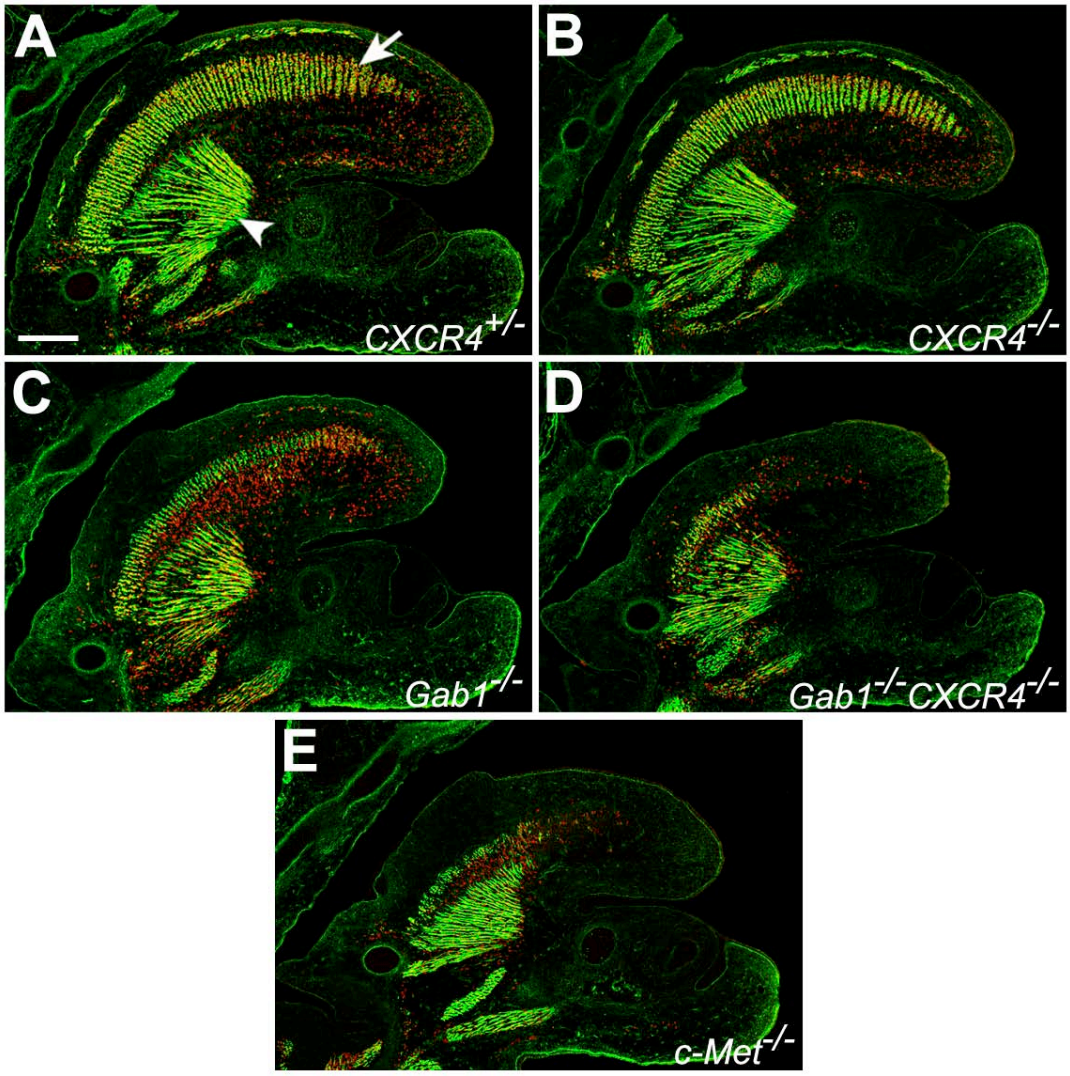

Figure 15. Differentiated muscle groups of the tongue.
(A-D) Sections of the tongue of *CXCR4*$^{+/-}$ (A), *CXCR4*$^{-/-}$ (B), *Gab1*$^{-/-}$ (C), *CXCR4*$^{-/-}$*Gab1*$^{-/-}$ (D) and *c-Met*$^{-/-}$ (E) embryos at E13.5 stained with antibodies to myosin (green) and MyoD (red). The intrinsic and extrinsic tongue muscles are indicated by an arrow and arrowhead in (A), respectively. Bar: 250 µm.

The extrinsic tongue muscle was not much changed in *Gab1* or *CXCR4;Gab1* mutant embryos compared to control mice (Fig. 15A,C,D).

In embryogenesis, the different muscles of the tongue originate from different types of cells. The proximal tongue muscle is mainly generated by head mesenchyme and only the distal part derives from long-range migrating muscle precursor cells (Huang et al. 1999). Consequently, the muscle deficit in the distal tongue is in agreement with impaired migration of muscle precursor cells along the hypoglossal stream at earlier developmental stages in *CXCR4;Gab1* double mutants. To validate this, the tongue muscles of $CXCR4^{-/-}Gab1^{-/-}$ and $c\text{-}Met^{-/-}$ mutant embryos were compared (Fig. 15D,E). In *c-Met* mutant embryos, muscle precursor cells fail to delaminate from the somites and consequently the particular muscle groups that are formed by migrating precursor cells are missing (Bladt et al. 1995; Dietrich et al. 1999). The appearance of the tongue muscle of *CXCR4;Gab1* mutant embryos is comparable to that observed in *c-Met* mutants. This supports the notion that muscle precursor cells do not contribute to the formation of tongue muscle in *CXCR4;Gab1* mutant embryos (Fig. 15D,E).